

## Spin Gratings and the Measurement of Electron Drift Mobility in Multiple Quantum Well Semiconductors

A. R. Cameron,\* P. Riblet, and A. Miller

The J. F. Allen Research Laboratories, School of Physics and Astronomy, University of St. Andrews, St. Andrews KY16 9SS, Scotland, United Kingdom

(Received 15 September 1995)

A direct optical measurement of electron drift mobility in multiple quantum well semiconductors is achieved by creating electron spin gratings in time-resolved degenerate four-wave mixing measurements. Grating decay rates are measured for spin and concentration gratings in a GaAs/AlGaAs sample at room temperature, giving an in-well electron diffusion coefficient  $D_e = 127 \text{ cm}^2/\text{s}$  compared with an ambipolar coefficient  $D_a = 13.3 \text{ cm}^2/\text{s}$ . [S0031-9007(96)00465-6]

PACS numbers: 73.20.Dx, 42.65.Hw, 42.65.Ky, 72.20.Fr

We report a new type of optically induced, transient diffraction grating based on the spatial modulation of electron spin in a room temperature multiple quantum well (MQW) semiconductor. It is shown that electron spin gratings decay on picosecond time scales due to both spin relaxation and electron diffusion. We demonstrate the measurement of in-well *electron* drift mobility in GaAs MQWs by time-resolved, degenerate four-wave mixing (DFWM) resulting from spin gratings. Previously, DFWM studies have been limited to measurements of only the *ambipolar* (combined electron and hole) diffusion coefficient which is dominated by the hole mobility. We compare the decay times of electron spin gratings and concentration gratings to give both electron and hole drift mobilities.

DFWM has been used extensively to probe semiconductors and other materials [1]. The use of three input beams consisting of ultrashort pulses from a mode-locked laser allows monitoring of the spatial dynamics of optically excited free carriers and excitons in semiconductors. Many recent short pulse DFWM studies of MQWs have addressed low temperature coherent phenomena involving excitons [2] and biexcitons [3], dephasing [4,5], reorientation [4], and localization [6,7]. Room temperature DFWM studies have concentrated on in-well carrier diffusion [8] and cross-well transport [8,9]. At room temperature, coherence is rapidly lost on femtosecond time scales due to scattering from phonons. The dominant excitonic optical nonlinearities result from the free carrier interactions, phase space filling (PSF), and Coulomb screening [10].

Gratings are formed in semiconductors when two non-collinear pulses interfere to produce a spatial modulation of the optical properties by carrier generation. A third, time-delayed pulse is diffracted from the temporary grating. Two types of interference of the optical pulses can be produced depending on the relative polarizations of the beams. An amplitude modulation results from two beams with *parallel* linear polarizations which creates a free carrier *concentration* grating in the material. This grating decays by a combination of carrier recombination and diffusion from regions of high to low population. Since equal

numbers of electrons and holes are generated, monitoring the grating decay for different grating spacings allows the ambipolar diffusion coefficient to be determined, and from this the hole diffusion coefficient can be estimated. This technique has been used to measure ambipolar diffusion coefficients in a number of semiconductors including GaAs MQWs [8]. An alternative optical technique is time of flight which has been used to determine exciton diffusion coefficients in MQWs [11].

When two beams with *crossed*-linear polarizations intersect, the light amplitude is uniform but the electric field polarization is spatially modulated across the excitation region. For equal excite intensities, the polarization changes from linear to circular to orthogonal linear to circular of the opposite sense and back to linear, as shown in Fig. 1(a). The period of this modulation is identical to that produced by amplitude gratings and is defined by the angle between the two excite beams and the wavelength of light used. The crossed-linear configuration has been used previously in semiconductors to observe anisotropic (i.e., wave-vector direction-dependent) state filling [12] or alignment of exciton dipoles [4,5] via the spatial modulation of the *linear* polarization. However, Fig. 1(a) shows that crossed-linear polarizations also produce a modulation in *circular* polarization. An alternative description of this polarization grating is obtained by separating it into two

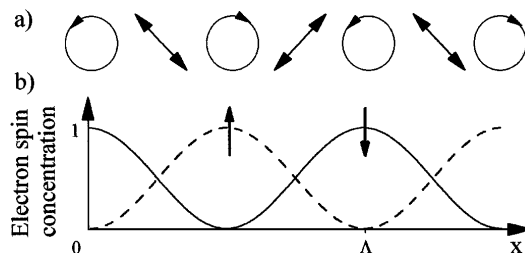


FIG. 1. (a) The polarization modulation produced when two orthogonally polarized light beams interfere. (b) Concentration of spin-up and spin-down electrons created by a polarization grating.

circularly polarized components with opposite directions of rotation [13]. The electric field modulation  $E(x)$  along the grating direction  $x$  can be written in terms of these two circular polarization components,

$$E(x) = E_0 \left\{ \sin\left(\frac{\pi x}{\Lambda}\right) e^{-i\pi/4} \frac{\hat{x} + i\hat{y}}{\sqrt{2}} + \cos\left(\frac{\pi x}{\Lambda}\right) e^{i\pi/4} \frac{\hat{x} - i\hat{y}}{\sqrt{2}} \right\} + \text{c.c.}, \quad (1)$$

where  $\Lambda$  is the grating spacing and  $\hat{x}$  and  $\hat{y}$  are unit vectors describing the polarization directions of the incident beams. Therefore, a nonlinearity which is sensitive to circular polarization will create a grating from two orthogonal linearly polarized beams.

In MQW semiconductors, lifting of the degeneracy between the light and heavy hole bands due to confinement allows access to polarization sensitive optical selection rules, Fig. 2. Circularly polarized light resonant with the heavy hole exciton generates 100% spin-polarized electron-hole pairs. The spin orientation is maintained by the electrons for tens of picoseconds after rapid ionization of the excitons by longitudinal optical phonons (within 300 fs at room temperature [14]). Hole spins may be expected to relax on subpicosecond time scales at room temperature because of band mixing and the mixed spin character of the valence states [15]. Thus excitation at the heavy hole exciton in a MQW with crossed-linear polarized pulses creates a spatial modulation of the electron spins, Fig. 1(b). At sufficient fluences, electrons saturate the exciton absorption via PSF and Coulomb screening [10]. It has been shown previously that the PSF contribution to exciton saturation is spin dependent [16]. Therefore, a spatial modulation of electron spin orientation will diffract a circularly polarized probe beam. Indeed, a linearly polarized probe beam will also be diffracted by this spin grating since both right and left circular components will be diffracted from the two opposite spin gratings.

The spin grating decay rate will be determined by a combination of the spin relaxation rate and diffusion of the electrons within the quantum wells. Since hole spin relaxation is rapid, washout of the spin grating can be interpreted in terms of the motion of electrons alone and

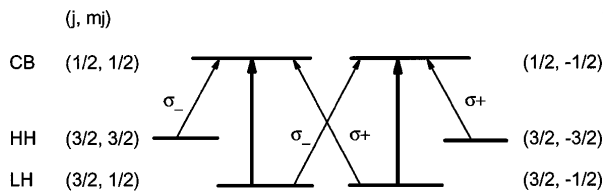


FIG. 2. The selection rules for the transitions from the heavy hole and light hole valence bands to the conduction band in MQWs. The  $(j, m_j)$  refer to the quantum numbers for angular momentum and its component along one direction. The  $\sigma^+$  and  $\sigma^-$  refer to the transitions excited by each sense of circularly polarized light and correspond to  $\Delta m_j = \pm 1$ , respectively, where the propagation direction is used to define  $m_j$ .

the decay rate can be written

$$\Gamma = \frac{4\pi^2 D_e}{\Lambda^2} + \frac{1}{\tau_s}, \quad (2)$$

where  $D_e$  is the electron diffusion coefficient and  $\tau_s$  is the electron spin relaxation time. This expression is the same as that for a concentration grating, where the diffusion coefficient and lifetimes would be replaced by  $D_a$ , the ambipolar diffusion coefficient, and  $\tau_R$ , the recombination time for electrons and holes.

DFWM experiments were carried out using a self-mode-locked Ti:sapphire laser (Spectra-Physics, Tsunami) producing  $\sim 1$  ps pulses at 82 MHz. Two pump beams and a time delayed probe beam were configured in a standard forward traveling geometry so that the grating modulation was produced in the plane of the quantum wells. The polarization of one of the pump beams was rotated by  $90^\circ$  to allow the creation of the polarization grating. The average power in the pump beams was  $500 \mu\text{W}$  with  $\sim 50 \mu\text{W}$  in the probe beam. The spot sizes on the sample were  $30 \mu\text{m}$  (FWHM).

The sample KLB269 was grown by molecular beam epitaxy (MBE) and consists of 120 periods of  $65 \text{ \AA}$  GaAs quantum wells separated by  $21.2 \text{ nm}$   $\text{Al}_{0.4}\text{Ga}_{0.6}\text{As}$  barriers. The background doping was  $p \sim 10^{16} \text{ cm}^{-3}$ . The GaAs substrate was removed, an antireflection coating was applied to both surfaces, and the structure was mounted on a sapphire base for mechanical stability and heat sinking. The heavy and light hole exciton resonances were clearly resolved at 1.494 and 1.51 eV, respectively. Previous amplitude grating studies on this sample [8] have shown that the peak diffraction efficiency occurs on the long wavelength side of the heavy hole exciton since the grating is refractive. Excitation at this energy results in the production of excitons which are rapidly ionized. Thus on the time scale of the experiments described here ( $> 1$  ps), optically generated carriers occupy the states at the top (bottom) of the valence (conduction) bands. Miller *et al.* [8] have measured a room temperature recombination time of 70 ns for this sample.

The electron spin relaxation time  $\tau_s$  can be determined from time-resolved measurements of exciton saturation employing two circularly polarized beams [16,17]. Figure 3 shows the probe transmission change as a function of delay under three different polarization combinations of pump and probe. Since PSF is enhanced by spin orientation when the same sense of circular polarization (SCP) of pump and probe is used, and reduced when opposite circular polarizations (OCP) are used, a spin relaxation time  $\tau_s = 55$  ps can be deduced from the recovery to the linear-linear (OLP) condition.

Figure 4 compares the diffracted probe signals for spin and concentration gratings produced at the heavy hole exciton using crossed- and parallel-linear polarized pump pulses, respectively. The probe was linearly polarized in both cases. The polarization of the diffracted beam from

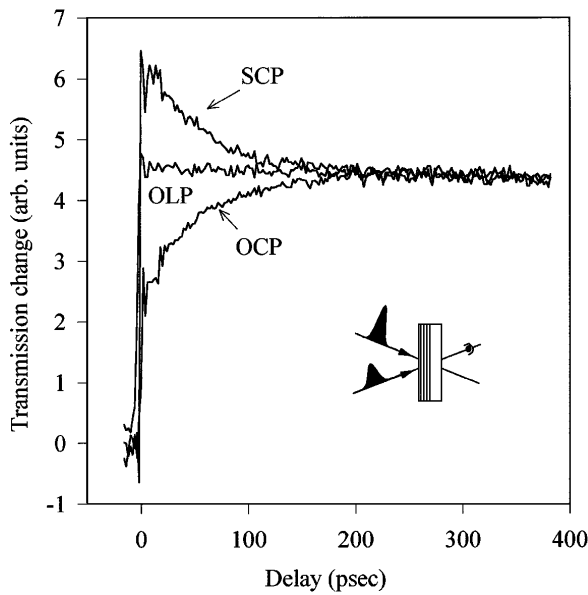


FIG. 3. The dependence of probe transmission change on optical time delay in pump-probe measurements for three polarization configurations: OLP = opposite linear polarization, SCP = same circular polarization, OCP = opposite circular polarization.

the spin grating was observed to be rotated by 90°, as predicted by the  $\pi$  phase shift between the spin-up and spin-down grating components, Fig. 1. The diffracted probe signals for spin and concentration gratings are characterized by single exponential decays with the spin grating

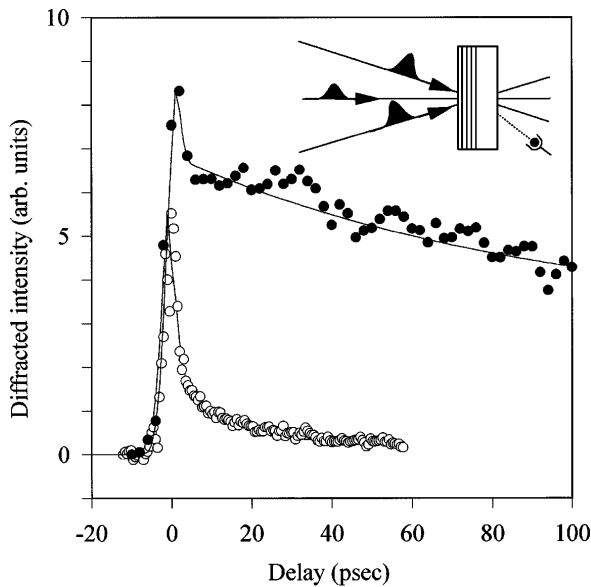


FIG. 4. The measured diffracted signal decay rate for a 5  $\mu\text{m}$  concentration amplitude grating (●) compared with the corresponding 5  $\mu\text{m}$  electron spin grating (○). Exponential decays with time constants of 220 and 13 ps are fitted to the two grating signals.

showing a much faster decay rate. The estimated excess carrier density for the spin grating was  $\sim 5 \times 10^{16} \text{ cm}^{-3}$ . The long carrier lifetime of the sample creates a background carrier population which does not effect the decay times since no intensity dependence of the decay rates was observed at this excitation level. Coherence spikes at zero delay in both decay curves are attributed to diffraction of one pump beam from a grating created between the probe and the other pump beam.

The decay rates ( $2\Gamma$ ) of the diffracted signal obtained for a number of spin and concentration grating periods  $\Lambda$  are plotted in Fig. 5. The spin relaxation result  $\tau_s = 55 \text{ ps}$  is included in Fig. 5 as the infinite grating spacing limit. The ambipolar,  $D_a$ , and electron,  $D_e$ , diffusion coefficients can be deduced from the gradients [Eq. (2)]. A value of  $D_a = 13.3 \text{ cm}^2/\text{s}$  is in good agreement with previous studies [8]. The deduced hole mobility of  $\mu_h \sim 257 \text{ cm}^2/\text{V s}$  is in excellent agreement with values for GaAs.

The spin grating results give a diffusion coefficient of  $D_e = 127 \text{ cm}^2/\text{s}$ . The electron drift mobility is derived from this diffusion coefficient using the Einstein equation in the usual way, since the mean free path of the electrons is the same whether there is an overall density gradient or a gradient only in spin concentration. The electron drift mobility deduced in this way is  $\mu_e = 4924 \text{ cm}^2/\text{V s}$ . This value is lower than the typical room temperature value of  $8500 \text{ cm}^2/\text{V s}$  for pure bulk GaAs; however, the difference can be attributed to the high background doping of the sample used here. Ionized impurity scattering significantly affects the electron mobility [18]. Taking into account the background doping, a mobility of  $\sim 6000 \text{ cm}^2/\text{V s}$  may be expected in bulk GaAs. A fur-

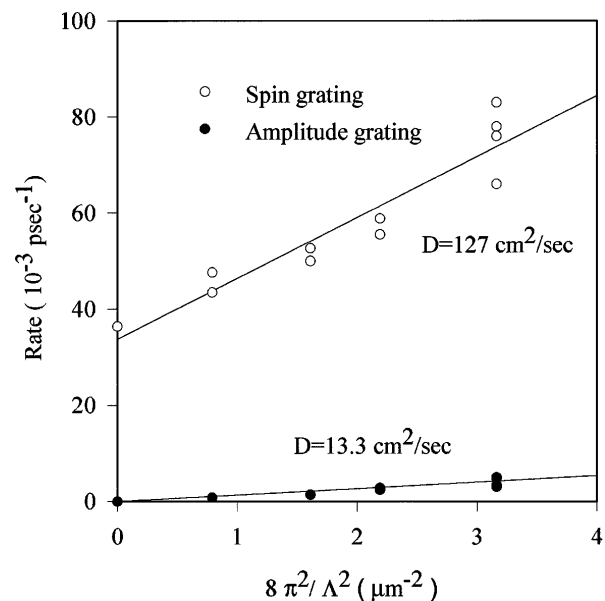


FIG. 5. Measured decay rates of the diffracted grating signal against  $8\pi^2/\Lambda^2$ . Amplitude grating results (●) and spin grating results (○) are plotted together for comparison.

ther decrease may be attributed to interface scattering within the quantum well layers.

In conclusion, we have demonstrated electron spin gratings in DFWM for the first time and directly measured the electron drift mobility in GaAs/AlGaAs MQWs at room temperature by time resolving the motion of spin-polarized electrons within the quantum well layers. A 90° rotation of the linear polarization of the diffracted probe beam is consistent with two phase-shifted spin gratings with opposite spin. Possible uses of electron spin gratings are the study of high electron mobility transistor (HEMT) structures and probing of spin relaxation processes. Measurement of the diffraction efficiencies from MQW spin gratings will allow characterization of recently demonstrated all-optical switches in MQWs based on circularly polarized light [19]. From a nonlinear optical device standpoint, we note that the DFWM signal is observed at relatively low intensities,  $\sim 200 \text{ kW/cm}^2$  (compared to  $> 1 \text{ GW/cm}^2$  in orientational gratings produced by anisotropic state filling), because of the resonant exciton nonlinearity, while the time constant is still relatively fast ( $< 100 \text{ ps}$ ).

This work was supported by the Engineering and Physical Sciences Research Council. We are grateful to David Hutchings, Michael Snelling, and Peggy Perozzo for valuable discussions and Karl Woodbridge for the MQW sample.

---

\*Electronic address: arc@st-andrews.ac.uk

- [1] H. M. Van Driel, in *Nonlinear Optical Materials and Devices for Applications in Information Technology*, edited by A. Miller, K. R. Welford, and B. Daino, NATO ASI, Ser. E, Vol. 289 (Kluwer, Dordrecht, 1995).
- [2] K. Leo, E. O. Göbel, T. C. Damen, J. Shah, S. Schmitt-Rink, W. Schäfer, J. F. Muller, K. Köhler, and P. Ganser, *Phys. Rev. B* **44**, 5427 (1991).
- [3] D. S. Kim, J. Shah, T. C. Damen, L. N. Pfeiffer, and W. Schäfer, *Phys. Rev. B* **50**, 5775 (1994).
- [4] L. M. Schultheis, J. Kuhl, A. Honold, and C. W. Tu, *Phys. Rev. Lett.* **57**, 1797 (1986).
- [5] S. T. Cundiff, H. Wang, and D. G. Steel, *Phys. Rev. B* **46**, 7248 (1992).
- [6] J. Hegarty and M. D. Sturge, *J. Opt. Soc. Am. B* **2**, 1143 (1985).
- [7] R. Hellmann, S. T. Cundiff, M. Koch, J. Feldmann, E. O. Göbel, B. Kuhn-Heinrich, D. R. Yakovlev, A. Waag, and G. Landwehr, *Phys. Rev. B* **50**, 14 651 (1994).
- [8] A. Miller, R. J. Manning, P. K. Milsom, D. C. Hutchings, D. W. Crust, and K. Woodbridge, *J. Op. Soc. Am. B* **6**, 567 (1989).
- [9] D. P. Norwood, H. E. Swoboda, M. D. Dawson, A. L. Smirl, D. R. Anderson, and T. C. Hasenberg, *Appl. Phys. Lett.* **59**, 219 (1991); D. P. Norwood, A. L. Smirl, and H.-E. Swoboda, *J. Appl. Phys.* **77**, 1113 (1995).
- [10] S. Schmitt-Rink, D. S. Chemla, and D. A. B. Miller, *Phys. Rev. B* **32**, 6601 (1985).
- [11] H. Hillmer, A. Forchel, S. Hansmann, M. Morohashi, E. Lopez, H. P. Meier, and K. Ploog, *Phys. Rev. B* **39**, 10 901 (1989).
- [12] A. L. Smirl, T. F. Boggess, B. S. Wherrett, G. P. Perryman, and A. Miller, *Phys. Rev. Lett.* **49**, 933 (1982).
- [13] T. S. Rose, W. L. Wilson, G. Wackerle, and M. D. Fayer, *J. Phys. Chem.* **91**, 1704 (1987).
- [14] W. H. Knox, R. L. Fork, M. C. Downer, D. A. B. Miller, D. S. Chemla, C. V. Shank, A. C. Gossard, and W. Weigmann, *Phys. Rev. Lett.* **54**, 1306 (1985).
- [15] R. Ferreira and G. Bastard, *Phys. Rev. B* **43**, 9687 (1991).
- [16] M. J. Snelling, P. Perozzo, D. C. Hutchings, I. Galbraith, and A. Miller, *Phys. Rev. B* **49**, 17 160 (1994).
- [17] S. Bar-Ad and I. Bar-Joseph, *Phys. Rev. Lett.* **68**, 349 (1992).
- [18] S. M. Sze, *Physics of Semiconductor Devices* (Wiley, New York, 1981), 2nd ed.
- [19] Y. Nishikawa, A. Tackeuchi, S. Nakamura, S. Muto, and N. Yokoyama, *Appl. Phys. Lett.* **66**, 839 (1995).